Biochimica et Biophysica Acta 1807 (2011) 1237–1243

Contents lists available at ScienceDirect

Biochimica et Biophysica Acta

journal homepage: www.elsevier.com/locate/bbabio

Light-induced isomerization of the LHCII-bound xanthophyll neoxanthin: Possible implications for photoprotection in plants

Monika Zubik [a,1], Rafał Luchowski [a], Wojciech Grudzinski [a], Małgorzata Gospodarek [b], Ignacy Gryczynski [c], Zygmunt Gryczynski [c,d], Jerzy W. Dobrucki [e], Wiesław I. Gruszecki [a,*,1]

[a] Department of Biophysics, Institute of Physics, Maria Curie-Sklodowska University, 20–031 Lublin, Poland
[b] Department of Biophysics, Medical University, Lublin, Poland
[c] Center for Commercialization of Fluorescence Technologies, University of North Texas Health Science Center, Fort Worth TX, USA
[d] Department of Physics and Astronomy, Texas Christian University, Fort Worth TX, USA
[e] Laboratory of Cell Biophysics, Faculty of Biochemistry, Biophysics and Biotechnology, Jagiellonian University, Krakow, Poland

ARTICLE INFO

Article history:
Received 19 April 2011
Received in revised form 13 June 2011
Accepted 15 June 2011
Available online 22 June 2011

Keywords:
Photosynthesis
Photoprotection
Xanthophyll
Spectroscopy
Fluorescence
LHCII

ABSTRACT

Light-harvesting pigment-protein complex of Photosystem II (LHCII) is the largest photosynthetic antenna complex of plants and the most abundant membrane protein in the biosphere. Plant fitness and productivity depend directly on a balance between excitations in the photosynthetic apparatus, generated by captured light quanta, and the rate of photochemical processes. Excess excitation energy leads to oxidative damage of the photosynthetic apparatus and entire organism and therefore the balance between the excitation density and photosynthesis requires precise and efficient regulation, operating also at the level of antenna complexes. We show that illumination of the isolated LHCII leads to isomerization of the protein-bound neoxanthin from conformation 9′-*cis* to 9′,13- and 9′,13′-*dicis* forms. At the same time light-driven excitation quenching is observed, manifested by a decrease in chlorophyll *a* fluorescence intensity and shortened fluorescence lifetimes. Both processes, the neoxanthin isomerization and the chlorophyll excitation quenching, are reversible in dim light. The results of the 77 K florescence measurements of LHCII show that illumination is associated with appearance of the low-energy states, which can serve as energy traps in the pigment–protein complex subjected to excess excitation. Possible sequence of the molecular events is proposed, leading to a protective excess excitation energy quenching: neoxanthin photo-isomerization → formation of LHCII supramolecular structures which potentiate creation of energy traps → excitation quenching.

1. Introduction

Life on our Planet is powered by the energy of the Sun and photosynthesis is practically the sole process enabling the transformation of solar energy into forms which can be utilized directly by living organisms. On one hand, a low level of excitations, in the photosynthetic apparatus of plants, may appear not sufficient to maintain metabolism but, on the other hand, overexcitation can lead to generation of reactive oxygen species, damage of the photosynthetic apparatus and eventually death of the plant. During evolution, plants developed multiple regulatory mechanisms, operating at all the organizational levels of organisms to balance excitation density in the photosynthetic apparatus with respect to capacity of the photochemical reactions. Among such regulatory mechanisms are the: movements of leaves [1], translocation of chloroplast in the cell [2], migration [3] and reorganization [4] of antenna proteins in the thylakoid membranes and regulation of the excitation density at the level of the reaction centers and antenna complex network, e.g. manifested by chlorophyll *a* fluorescence variations in intact leaves [5]. Interestingly, it appears that such a kind of regulation can be also attributed to single pigment-protein antenna complexes. Illumination of isolated antenna complex LHCII results in the development of singlet excitation quenching, which is dark reversible [6–8]. Isolated complex seems to be a very good model of a photosynthetic antenna under overexcitation conditions, since it does not have a possibility of transferring excitations out of it, towards the reaction centers. Interestingly, it has been demonstrated recently, using single-molecule fluorescence spectroscopy, that isolated trimeric LHCII is able to modulate dynamically fluorescence intensity and shift emission wavelengths towards low-energy spectral regions [9]. Despite a general agreement regarding the importance of excitation quenching within single antenna complexes, there are several concepts on exact molecular mechanism(s) responsible for such a quenching. In most cases, the concepts proposed are contradictory and mutually exclusive and therefore this issue seems to be not only the important one and interesting but also requiring further examination and discussion. Ruban and coworkers have demonstrated that the transition into the

* Corresponding author. Tel.: +48 81 537 62 52; fax: +48 81 537 61 91.
E-mail address: wieslaw.gruszecki@umcs.pl (W.I. Gruszecki).
[1] These authors contributed equally to this work.

0005-2728/$ – see front matter © 2011 Elsevier B.V. All rights reserved.
doi:10.1016/j.bbabio.2011.06.011

dissipative state is associated with a twist in the configuration of the LHCII-bound carotenoid neoxanthin [10]. The authors have proposed the molecular events cascade, linking causatively the light-induced change in neoxanthin configuration and the excitation quenching via induced shortening of the distance between one lutein and chlorophyll molecules, followed by chlorophyll singlet excitation quenching by this xanthophyll [10]. On the other hand, such a concept has been questioned for two reasons. Firstly, the protein does not demonstrate enough flexibility to allow for the hypothesized intermolecular distance changes [11,12] and secondly, it has been shown that singlet energy dissipation in LHCII does not involve energy transfer to carotenoids [13]. Another line of interpretation of excess excitation energy quenching in the photosynthetic pigment-protein antenna complexes is based upon formation of a zeaxanthin–chlorophyll charge transfer complex enabling chlorophyll singlet excitation quenching [14]. The possibility of such energy dissipation pathway has been, however, questioned on the bases of theoretical calculations [15] and spectroscopic studies with application of the two color two photon ionization spectroscopy [16]. On the other hand, direct quenching of chlorophyll excited states by energy transfer to carotenoid cation radicals has been shown to be possible and efficient [17]. Very recently we have found that illumination of the isolated LHCII with blue light, absorbed both by chlorophylls and xanthophylls, drives chlorophyll *a* singlet excitation quenching much more efficiently than in the case of illumination with red light, absorbed exclusively with chlorophylls, despite the equalized absorbed energy [18,19]. Such an effect suggests a specific role of the LHCII-bound xanthophylls in excess excitation energy quenching. It is very likely that multiple mechanisms leading to quenching of excess excitations operate parallel and independently at the molecular level. Among such mechanisms most often discussed are the ΔpH-dependent quenching and the xanthophyll cycle-dependent quenching (see [20] for most recent review). In the present work we address the problem of light-induced excitation quenching in LHCII which is energetically uncoupled from PSII, as for example under the state transition conditions. The mechanisms of light-driven singlet excitation quenching in isolated LHCII can account for more than 30% excitation quenching [8]. Singlet excitation quenching prevents generation of the chlorophyll triplets and sensitized formation of the singlet oxygen and therefore can be considered as an important component of overall photoprotection at the molecular level of the single antenna pigment-protein complex.

2. Materials and methods

2.1. Isolation and purification of LHCII and neoxanthin

The major light-harvesting pigment-protein complex of Photosystem II (LHCII) was isolated from fresh spinach leaves according to [21]. The complex's integrity and purity were confirmed by means of electrophoresis, HPLC, and mass spectrometry as described previously [22]. All the chemicals used in the preparation of the buffer solution were purchased from Sigma Chem. Co. (USA). The protein was suspended in Tricine buffer (20 mM, pH, 7.6, 10 mM KCl). Neoxanthin was isolated from spinach leaves as described previously [23,24] and purified chromatographically (HPLC, described later).

2.2. Preparation of proteoliposomes

Monogalactosyldiacylglycerol (MGDG) and Digalactosyldiacylglycerol (DGDG) were purchased from Lipid Products Company (Redhill UK). Liposomes containing lipids MGDG and DGDG in molar ratio respectively 2:1 were prepared and LHCII was incorporated according to the following protocol. The glass test tubes containing lipid film deposited via evaporation from the stock solution in chloroform under a stream of nitrogen were under reduced pressure (less than 10^{-5} bar) kept for 30 min in order to remove the remaining solvent. The lipids were suspended in the buffer (Tricine 20 mM, pH, 7.6, 10 mM KCl) and sonicated for 3 s with an ultrasound disintegrator UD-20 (Techpan, Poland) at a frequency of 22 kHz and an amplitude of 1–8 μm. LHCII suspended in the buffer was transferred to the liposome solution and vortexed vigorously for 30 min, centrifuged in two steps. The supernatant from the first centrifugation (1 min at 4400 ×*g*, in order to collect aggregated LHCII which did not incorporate to lipid bilayer) was centrifuged for 30 min at 11200 ×*g* (5 °C). The pellet was suspended in the buffer to obtain proteoliposome sample for analysis. The incorporated LHCII to lipid ratio was typically close to a value of 1 to 7700.

2.3. Light-induced isomerization of neoxanthin

Light-induced pigment isomerization was induced by illumination with blue light from a halogen illuminator combined with Schott BG12 band-pass filter 350–500 nm (light intensity 390 μmol m^{-2} s^{-1}). Neoxanthin was diluted in a solvent mixture: acetonitrile/methanol/water (72:8:3, v/v) to achieve an absorbance level of 0.5 (optical path length 1 cm) and deoxygenated by bubbling with a gaseous argon for 5 min. During illumination the sample was continuously stirred with a magnetic stirrer. The same experiment was carried out with the LHCII samples suspended in the buffer. Pigment chromatographic analyses (HPLC, described later) were done immediately after illumination. LHCII pigments were extracted in a solvent mixture: acetonitrile/methanol (72:8, v/v).

2.4. HPLC analysis

High performance liquid chromatography (HPLC) analyses were carried out on a C-30 coated, phase-reversed column from YMC GmbH, Germany (length 250 mm, internal diameter 4.6 mm) with the following solvent system: acetonitrile/methanol/water (72:8:3, v/v), which was used as a mobile phase. The HPLC elution rate was 1,5 ml/min. A diode-array Hewlett-Packard spectrophotometer, model HP 8453, was used as a detector, to record absorption spectra between 200 and 800 nm in 10 s intervals.

2.5. Steady-state fluorescence spectroscopy

77 K fluorescence excitation and emission spectra were recorded on a Cary Eclipse (Varian Inc., Australia) fluorescence spectrophotometer with the system described previously [25]. The excitation and emission monochromator slits were set to a bandpass of 10 nm. The spectra were corrected for the lamp intensity. Fluorescence decay kinetics were analyzed at room temperature with excitation at 470 nm (excitation and emission slits set to a bandpass of 5 nm) and at 635 nm (excitation and emission slits set to a bandpass of 20 nm and 1.5 nm, respectively). Different settings of the excitation monochromator slits were chosen in order to equalize absorbed light energy calculated on the basis of one-minus-transmission spectra of the LHCII samples and the exact intensity of excitation light beams at different wavelengths.

2.6. Fluorescence lifetime and FLIM measurements

Fluorescence lifetime imaging microscopy measurements were performed on a confocal MicroTime 200 (Picoquant, Germany) system coupled with an OLYMPUS IX71 microscope and a similar confocal system based on TCS SP5 X system (Leica Microsystems CMS, GmbH). Samples were placed on a non-fluorescent Menzel-Glaser #1 cover slips and mounted on a stage piezo-scanner. The fluorescence was excited by a solid state pulsed laser (635 nm and 470 nm with MT 200 and 476 nm with TCS SP5 X) with the repetition rate of 20 MHz. Fluorescence was observed through a 650 longpass filter in the MT 200 system and through 690/70 bandpass filter in the TCS SP5 X system. Fluorescence photons were collected with the Perkin-Elmer SPCM-AQR-14 single photon sensitive avalanche photodiode (APD)

and processed by the PicoHarp300 time-correlated single photon counting (TCSPC) module based on detection of photons of a periodical light signal. Decay data analysis was performed using SymPhoTime (v. 5.0) software package, which controlled the data acquisition as well.

2.7. Stark effect spectroscopy

Acquisition of the low temperature absorption and Stark spectra were performed on a home-build spectrometer equipped with a tungsten lamp and photodiode based detection system as described in detail previously [26,27]. The data for AC (field-induced modulation of transmitted light intensity) and DC (transmission) signals were collected simultaneously in 40 cm^{-1} steps. The sample diluted in water/glycerol (1/2 v/v) was measured in a frozen state, in a cryostat at 110 K.

The methodology used for Stark spectra analysis has already been described in detail elsewhere [28,29]. In short, the changes of absorbance ΔA caused by an external electric field F was approximated with two contributions proportional to the first and second derivative of absorption as follows:

$$\Delta A = \left(a_1 \upsilon \frac{d(A/\upsilon)}{d\upsilon} + a_2 \upsilon \frac{d^2(A/\upsilon)}{d\upsilon^2} \right) \times F^2 \quad (1)$$

Where a_1 and a_2 are proportional to the change of molecular polarizability Δα and square of permanent dipole moment Δμ.

2.8. Raman scattering spectroscopy

Raman scattering spectra from the liquid samples placed in the 0.2 mm quartz cuvettes were recorded with the inVia Reflex Raman Microscope from Renishaw (UK) equipped with two holographic ultra-high precision diffraction grating stages and high sensitivity ultra-low noise CCD detector. A 514.5 nm Ar^+ laser and an infrared 785 nm laser have been applied to record Raman scattering spectra. Laser power has been set to 8 mW. The spectra have been accumulated within 10 s integration time. The spectra were recorded at room temperature. The spectra were corrected by subtracting a background signal originating from fluorescence. To record Raman spectra neoxanthin was dissolved in ethanol and the solution was supplemented with glycerol (1:1, v:v).

Light-induced isomerization, and all spectroscopic measurements were performed at room temperature (25 ± 1 °C). All of the measurements were repeated at least six times and the effects presented were found to be reproducible.

2.9. Molecular modeling

Interaction of LHCII trimers was analyzed and visualized with VMD software support (http://www.ks.uiuc.edu/). VMD has been developed, with NIH support, by the Theoretical and Computational Biophysics group at the Beckman Institute, University of Illinois at Urbana-Champaign. LHCII coordinates were downloaded from the PDB database (PDB ID: 1RWT).

3. Results

Fig. 1 presents the neoxanthin elution profiles from the LHCII samples, dark adapted and subjected to illumination. As can be seen, despite a moderate illumination, neoxanthin present in LHCII in the 9′-*cis* geometrical isomeric form undergoes light-driven transformations to other forms, mostly 9′,13-*dicis* but also to the 9′,13′-*dicis* and all-*trans* forms (assignment based on [30]). Approximately 10% of the pigment pool has been light-transformed after the 10 min-illumination. As can be seen (Fig. 1), the illumination of the sample composed of pure isolated 9′-*cis* neoxanthin resulted in light-driven transformations, very similar to those observed in the case of LHCII. A longer light exposure (30 min) has led to comparable results (see Fig. S1 of the supplementary data) which means that under such light intensity, the light-driven isomerization and the reverse processes reached an equilibrium. Neoxanthin photo-isomerization can be followed in real time with application of continuous scanning in a diode-array spectrophotometer (see Fig. S2). In such experiment measuring light plays also a role of actinic light. Decreasing the intensity of measuring light resulted in a shift of equilibrium and a slow recovery of the light-driven process (see inset to Fig. S2).

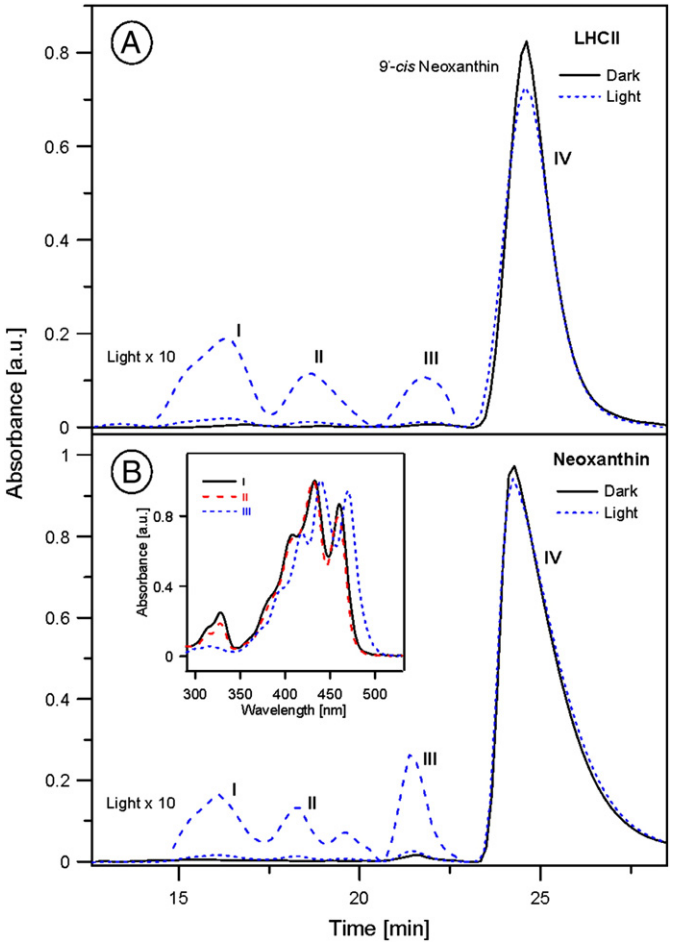

Fig. 1. (A) The HPLC elution profiles of neoxanthin extracted from LHCII, dark adapted (30 min) and illuminated for 10 min with blue light (350–500 nm, 390 μmol m^{-2} s^{-1}). Absorbance monitored at 441 nm. The chromatograms were calibrated with lutein (not shown). Assignment of the fractions based on [30]: I — 9′,13-*dicis*, II — 9′,13′-*dicis*, III — all-*trans*, IV — 9′-*cis*. (B) The HPLC elution profiles of the pure neoxanthin 9′-*cis* samples dark adapted (30 min) and illuminated for 10 min with blue light. Chromatograms were normalized with respect to a surface beneath each trace. The inset shows the normalized absorption spectra of the selected fractions, as indicated. The spectrum of the most common neoxanthin geometrical form (9′-*cis*, fraction IV) has not been shown for clarity of presentation. The spectroscopic parameters calculated on the basis of the absorption spectra are the following: Fraction I: III/II 70%, D_B/D_{II} 29%; fraction II: III/II 58%, D_B/D_{II} 19%; fraction III: III/II 85%, D_B/D_{II} 6%; fraction IV: III/II 96%, D_B/D_{II} 5%.

Illumination of the isolated LHCII, incorporated to liposomes, results in chlorophyll *a* fluorescence quenching, which is much more efficient in the case of the illumination with blue light as compared to the illumination with red light, despite equalized absorbed light energy (Fig. 2). Blue-light-driven chlorophyll *a* excitation quenching in LHCII embedded to liposomes is associated with fluorescence lifetime shortening (see Fig. 3) and the effect is reversible under relatively low light intensity conditions (see Fig. S3). Light-induced formation of supramolecular structures by LHCII has been demonstrated to induce

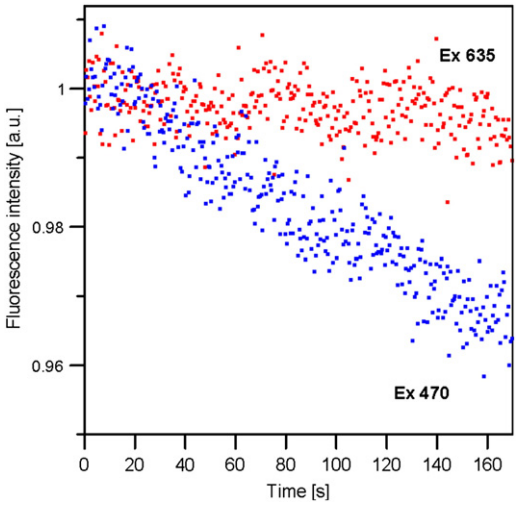

Fig. 2. Time dependencies of fluorescence intensity of chlorophyll *a* in LHCII incorporated to liposomes. Fluorescence intensity was recorded with a kinetic mode of the fluorescence spectrophotometer. The excitation was set either to 635 nm (red light-induced fluorescence quenching) or to 470 nm (blue light-induced fluorescence quenching) and fluorescence was detected at 680 nm, at the emission maximum of chlorophyll *a* in LHCII. Excitation light intensities have been modulated by means of combination of excitation slits (3–5 nm) and neutral filters to adjust the same energy absorbed by the sample in both cases. Fluorescence intensity was normalized at time zero.

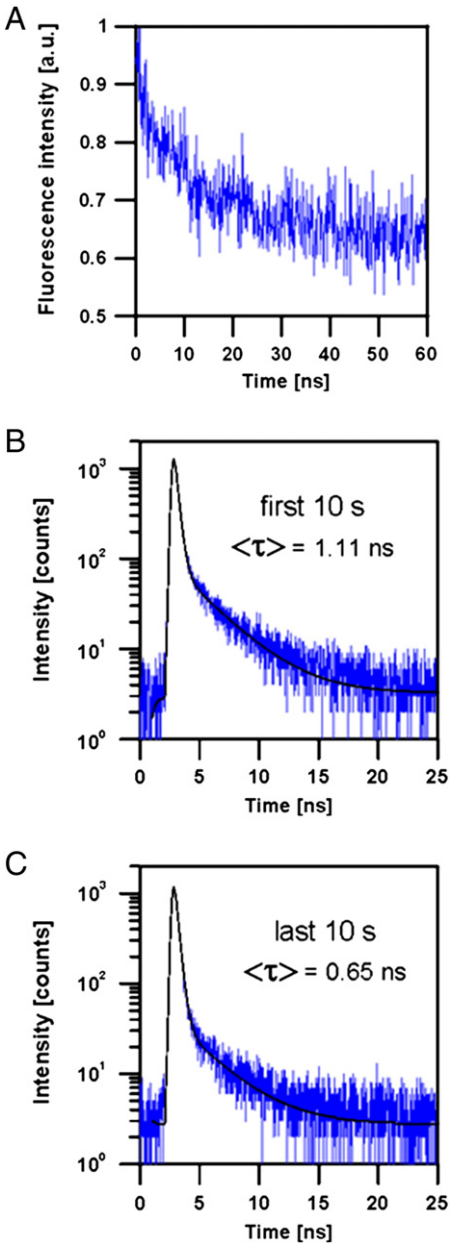

Fig. 3. (A) Time dependency of fluorescence intensity of chlorophyll *a* in LHCII incorporated to liposomes measured with FLIM technique with laser beam focused at a single selected liposome (see the supplementary information for images). Fluorescence decrease was induced by blue light laser (470 nm, 0.8 μW) and was detected after the 650 nm longpass filter. (B) Fluorescence lifetime analysis of the first 10 s of illumination (presented in panel A) and (C) the last 10 s of illumination. Intensity average lifetime values <τ> calculated for both illumination periods are also presented.

chlorophyll excitation quenching [31]. Formation of supramolecular structures of LHCII is also associated with remarkable changes in the low temperature fluorescence emission spectra of chlorophyll *a* [32,33]. Such spectral changes can be applied to monitor organization of LHCII, despite their exact nature (creation of new excitonic states versus fluorescence reabsorption [12]). Fig. 4 presents the 77 K chlorophyll *a* fluorescence emission spectra recorded from the liposome-embedded LHCII samples subjected to illumination with blue light and with red light. As can be seen from the difference spectrum, the blue-light-induced excitation quenching is associated with a slight bathochromic spectral shift of the main emission band and with appearance of new, low-energy levels manifested by the band centered at 693 nm and the broad emission band between 700 and 760 nm. Comparison of the low temperature absorption spectra recorded from the liposome-embedded LHCII, dark adapted and illuminated (see supplementary data Fig. S4), shows slightly increased absorption in the long-wavelength spectral region, characteristic of the absorption of chlorophyll and xanthophyll radicals. The Stark effect spectra of these long-wavelength bands show relatively small negative signals (see Fig. S5), analysis of which points into the light-induced reorganization of the pigment network, manifested by change in the electro-optical parameters. Changes in permanent dipole moment $\Delta\mu$ (1 D, calculated on the basis of the fit, Fig. S5) and in polarizability $\Delta\alpha$ 812 $Å^3$, in the illuminated sample, indicate that the long-wavelength transitions analyzed originate from hybrid, excitonic coupling and charge transfer, states. Since such a coupling is potentiated by illumination of the sample we propose a mechanism according to which the light-induced formation of new low-energy states is possible owing to assembly of individual LHCII trimers into supramolecular structures.

Fluorescence excitation spectra recorded from the same samples are presented in Fig. 5. Comparison of the difference fluorescence excitation spectrum with the difference absorption spectrum calculated from the neoxanthin solution in the 9′-*cis* and 9′,13-*dicis* forms suggests that the blue-light-induced spectral changes observed in the fluorescence spectra may, at last partially, be associated with neoxanthin photo-isomerization in LHCII, detected by means of the HPLC analysis (Fig. 1). The fact that this process can be observed in the chlorophyll *a* fluorescence excitation spectra can be accepted as an indication that the light-induced conversion of neoxanthin in LHCII is not associated with energetic uncoupling of this xanthophyll from the accessory pigment network in the antenna protein.

It is possible that the light-induced neoxanthin isomerization is a triplet-sensitized reaction [34]. Fig. 6 presents the Raman scattering spectra of 9′-cis neoxanthin, recorded in a resonance conditions, with excitation laser 514.5 nm, and with the 785 nm excitation laser, beyond the absorption band. As can be seen, the principal Raman band, corresponding to the C=C stretching modes (ν_1), is broadened and shifted towards lower frequencies, while recorded with strong probing light absorbed by the sample. The broadened band can represent appearance of additional species generated by light-

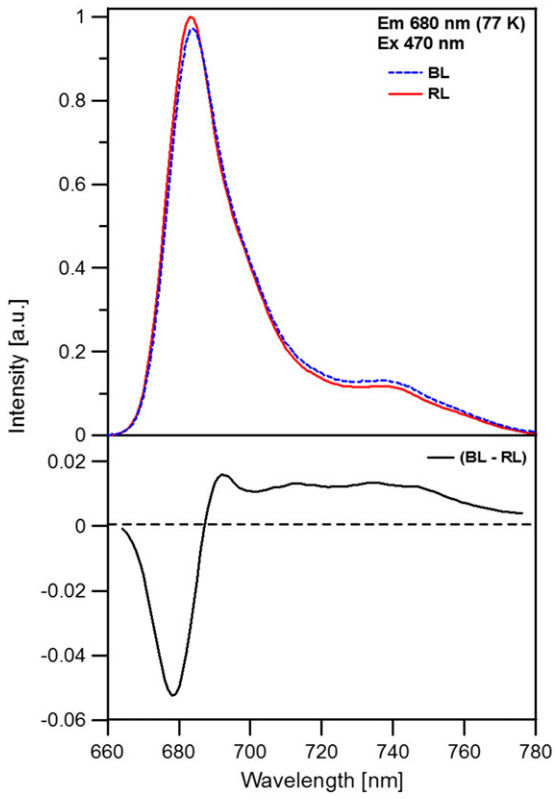

Fig. 4. The low temperature (77 K) chlorophyll *a* fluorescence emission spectra recorded from LHCII embedded to liposomes. Before measurements the samples were illuminated for 5 min with blue light (BL) or red light (RL) of the fluorescence spectrophotometer, under conditions the same as in the case of the experiment presented in Fig. 2. The spectra were normalized with respect to the surface area beneath the curves, in order to analyze spectral changes associated with the decreased fluorescence intensity. The lower panel shows the difference spectrum calculated on the basis of the spectra presented in the upper panel.

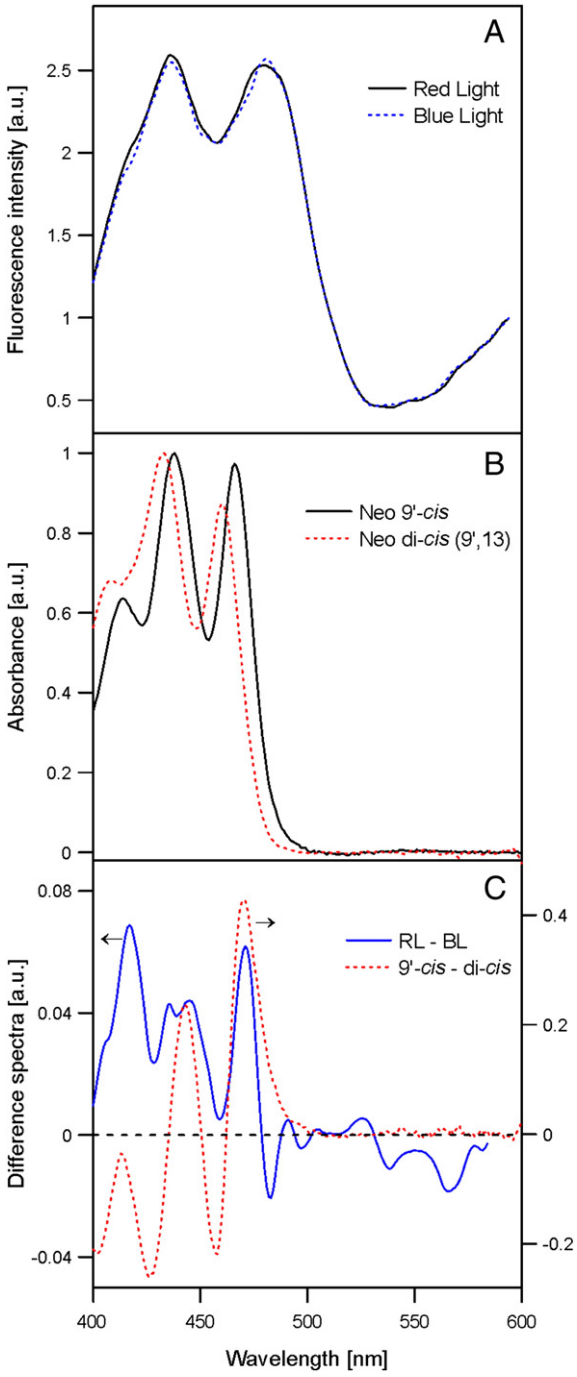

Fig. 5. (A) Low temperature (77 K) fluorescence excitation spectra of chlorophyll *a* in LHCII embedded to liposomes (emission detected at 680 nm). The spectra were normalized at 600 nm, in the spectral region corresponding to the absorption by chlorophylls, but not the carotenoids. Before measurements the samples were illuminated for 5 min with blue light (BL) or red light (RL) of the fluorescence spectrophotometer, under the same conditions as in the case of the experiment presented in Fig. 2. The excitation spectra were recorded from the same samples and correspond to the emission spectra presented in Fig. 4. (B) Normalized absorption spectra of neoxanthin in the geometrical isomeric form 9′-*cis* and 9′,13-*dicis* recorded in the solvent mixture acetonitrile/methanol/water (72:8:3, v/v). (C) A comparison between the difference spectra calculated on the basis of the spectra presented in panels a and b. The altered shape of the excitation spectra (as compared to trimeric LHCII) demonstrates supramolecular organization of LHCII in liposomes.

excitation. The fact that the new component is shifted, with respect to the main band position, towards lower frequencies suggests that it might be represented by a carotenoid in triplet excited state [34].

4. Discussion

Illumination of the isolated LHCII with laser light absorbed by the protein-bound xanthophylls gives rise to the resonance Raman spectroscopic effects which can be ascribed as monitoring the light-induced molecular configuration changes: to become more twisted in the case of neoxanthin (increase in intensity of the ν_4 band [10]) and an opposite effect observed, attributed to violaxanthin [22]. This latter effect, interpreted as liberation of the pigment from the protein bed, has been proposed to be involved in the process of making violaxanthin available for the enzymatic de-epoxidation, which takes place in the lipid phase of the thylakoid membrane [35]. In the present work we have applied the HPLC technique to analyze the effect of illumination on the molecular configuration of the LHCII-bound neoxanthin. The analyses revealed that certain fraction of neoxanthin, present initially in LHCII in the 9′-*cis* geometrical configuration, is transformed by a light-driven reaction to the other forms: 9′,13-*dicis*, 9′,13′-*dicis* and small fraction to the all-*trans*. According to integration of the spectra, the effective yield of light-induced neoxanthin isomerization in LHCII is ca. 10%. In our opinion the yield of this process is not high but substantial, taking into account that the back reaction is also observed under illumination conditions (Fig. S2). At the same time, under illumination conditions, the liposome-incorporated LHCII displayed the light-driven excitation quenching, monitored by chlorophyll *a* fluorescence decrease and shortening of the fluorescence lifetimes. LHCII has been incorporated to liposomes after vesicle preparation and the samples were separated from the protein aggregated structures, remaining in

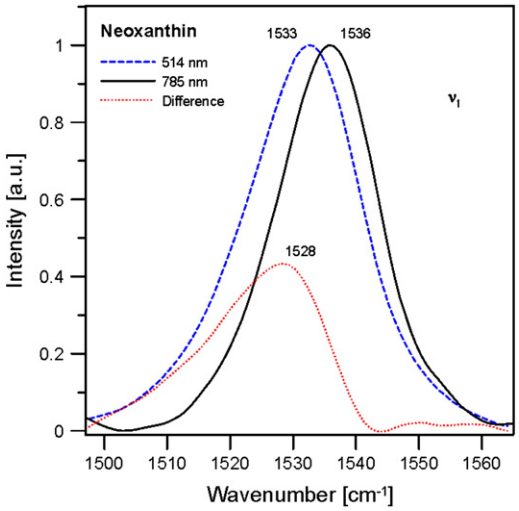

Fig. 6. Raman scattering spectra of 9′-cis neoxanthin recorded with lasers emitting light at 514.5 nm and 785 nm, indicated, presented in the ν_1 spectral region representing the C=C stretching modes. The spectra were normalized at the maximum. The difference spectrum is also presented calculated by subtracting the spectrum recorded with 785 nm laser and multiplied by a factor of 0.7 from the spectrum recorded with 514.5 nm laser. The factor has been selected to be as high as possible but not leading to a difference spectrum with negative components.

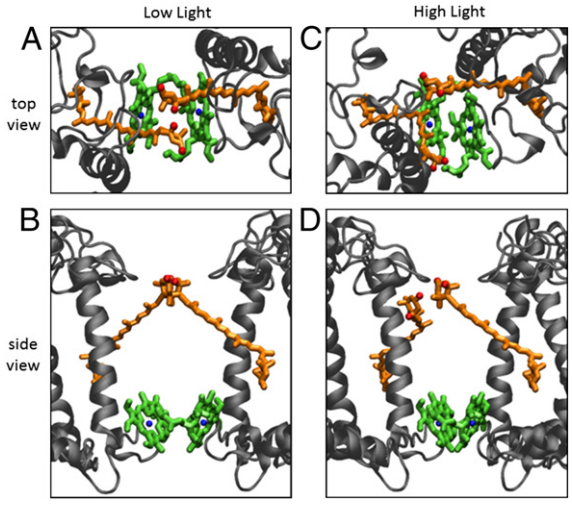

Fig. 7. Views of the molecular models of interaction of two LHCII trimers in the region of neoxanthin and the chlorophyll *b* (Chl 14, other pigments are not shown for clarity of presentation). A and C — top view, B and D — side view. The left hand side panels correspond to the complexes under physiological conditions, the right hand side panels correspond to excess illumination leading to neoxanthin photo-isomerization from the geometrical form 9′-*cis* to 9′,13-*dicis*. In panels a,b the distance between the Mg atoms in the center of neighboring chlorophyll molecules is 10.61 Å and in panels c,d this distance is 7.52 Å. In the latter case the chlorophyll molecules remain practically in the van der Waals contact, which enables intermolecular charge transfer. The distance between the oxygen atoms at position C5 of neighboring neoxanthin molecules in panels a,b is 2.7 Å, which enables hydrogen bond formation between the hydroxyl groups. The images were created with the VMD software support. VMD is developed with NIH support by the Theoretical and Computational Biophysics group at the Beckman Institute, University of Illinois at Urbana-Champaign. LHCII coordinates were downloaded from the PDB database (PDB ID: 1RWT).

the water phase. Such aggregates of LHCII are very efficient in chlorophyll fluorescence quenching (see Fig. S6), but rather unlikely to be formed in vivo, owing to a uniform (unidirectional) orientation of the complex in the thylakoid membrane [11]. The exceptional effect of blue light in driving the excitation quenching in LHCII, demonstrated also previously in other systems, with application of the fluorescence lifetime measurements [18,19], points directly to a central role of the LHCII-bound xanthophylls as photoreceptors responsible for triggering this effect. Light-driven excitation quenching in liposome-embedded LHCII is also associated with appearance of the low-wavelength fluorescence emission bands. As proposed recently, the appearance of the low-energy fluorescence emission bands of chlorophyll in LHCII can be directly responsible for the protective excess excitation energy dissipation in plants and associated with intermolecular interactions between the protein trimers [36]. The fact that the light-induced neoxanthin isomerization is observed in parallel to the light-induced excitation quenching and that both processes are driven preferentially by blue light suggests causative relationship between those mechanisms. Establishing of excitonic and/or charge transfer interactions could be, for example, possible by approaching the porphyrin rings of chlorophyll *b* molecules referred to as 605, in the terminology of Liu et al. [37], or Chl 14, in the terminology of Standfus et al. [38]. The analysis of the molecular structure of LHCII [37,38] shows, however, that close contact of those chlorophyll molecules is not possible due to the steric hindrance of neoxanthin molecules protruding out of the protein and, in particular, owing to hydrogen bond formations between the hydroxyl groups located at the positions C5 of neighboring neoxanthin molecules (see Fig. 7). On the other hand, light-induced isomerization of at least one neoxanthin from the geometrical form 9′-*cis* to the 9′,13-*dicis* will open possibility of such an interaction. The model based on such mechanism is presented in Fig. 7. As demonstrated earlier, the most effective pathway of the 9′-*cis* neoxanthin photo-isomerization leads to the formation of the *dicis* geometrical isomers. Moreover, this process is reversible under low light conditions, which provides opportunity for the neoxanthin photo-isomerization to play a role of a regulatory mechanism in plants subjected to light stress (reversibility under physiological conditions). The fact that neoxanthin isomerization can be a triplet-sensitized reaction, as concluded on the basis of Raman spectroscopy analysis, seems to make this mechanism particularly suited to play biological role in protection against light-induced damage. This is owing to the fact that triplet excitations are very efficiently accepted by carotenoids from chlorophylls and that chlorophyll triplet states in the photosynthetic antenna complexes are only expected to be present under overexcitation conditions. However, as demonstrated by Mozzo et al., 95% of chlorophyll triplet excitations are quenched by lutein molecules, placed in the central part of the complex [39]. On the other hand, it is possible that neoxanthin triplets can be also formed via singlet oxygen quenching. Singlet oxygen in the neighborhood of LHCII can be generated with collisions of molecular oxygen with triplet excited chlorophylls which are not quenched by lutein (ca. 5%). The observation that neoxanthin photo-isomerization is more efficient in LHCII than in the sample of isolated pigments, under comparable illumination conditions (Fig. 1), supports such a hypothesis. It has to be noted that generation of carotenoid triplet states via triplet-triplet energy transfer or collisions with singlet oxygen is much more efficient than via intersystem crossing from singlet excited states [40].

Interestingly, it has been demonstrated that the *Arabidopsis* aba4-1 mutant, lacking neoxanthin, was more sensitive than the wild type to light stress [41]. The neoxanthin site in LHCII can be also occupied by the 9-*cis* violaxanthin [41,42] but photo-isomerization of violaxanthin does not lead to substantial accumulation of *dicis* geometrical forms [25], contrary to neoxanthin, as demonstrated earlier.

5. Conclusions

We propose the presence of a regulatory mechanism in the photosynthetic apparatus of plants subjected to excess excitation energy supply. The mechanism is based upon interaction of LHCII trimers, leading to the creation of low-energy traps. According to our interpretation of the experimental results, the strong-light-induced isomerization of the LHCII-bound xanthophyll neoxanthin, to a *dicis* geometrical configuration, removes steric hindrance and hydrogen bonding between neoxanthin molecules bound to the neighboring LHCII trimers and enables them to approach to a distance which results in establishing excitonic interactions

and charge transfer complexes between the peripheral chlorophyll molecules. In our opinion, such a coupling gives rise to low-energy levels — traps acting to quench singlet excitations in the antenna complex. All the mechanisms proposed have been demonstrated in the present work to operate in the model system based on LHCII embedded to liposomes. We expect that owing to the considerable molecular crowding of LHCII in the thylakoid membranes [43,44] the light-driven excitation quenching, induced by inter-trimer interaction will take place on a considerably larger scale. Additionally, light-induced isomerization of neoxanthin, provides potential conditions for close coupling between the Chl 14 and other peripheral chlorophyll molecules, from the pigment-protein complexes other than LHCII, situated on the energy transfer pathways closer to the PS II reaction center.

Acknowledgements

The authors wish to thank Prof. Stanislaw Krawczyk for making available the Stark effect experimental set-up and expertise advices. This research was financed by the Ministry of Science and Higher Education of Poland from the funds for science in the years 2008–2011 within the research project N N303 285034. ZG acknowledges the financial support from NIH (R01EB012003).

Appendix A. Supplementary data

Supplementary data to this article can be found online at doi:10.1016/j.bbabio.2011.06.011.

References

[1] M.L. Stanton, C. Galen, Blue light controls solar tracking by flowers of an alpine plant, Plant Cell Environ. 16 (1993) 983–989.
[2] H. Gabrys, Blue light-induced orientation movements of chloroplasts in higher plants: recent progress in the study of their mechanisms, Acta Physiol. Plant. 26 (2004) 473–478.
[3] J.F. Allen, State transitions — a question of balance, Science 299 (2003) 1530–1532.
[4] G. Garab, Z. Cseh, L. Kovacs, S. Rajagopal, Z. Varkonyi, M. Wentworth, L. Mustardy, A. Der, A.V. Ruban, E. Papp, A. Holzenburg, P. Horton, Light-induced trimer to monomer transition in the main light- harvesting antenna complex of plants: thermo-optic mechanism, Biochemistry 41 (2002) 15121–15129.
[5] M. Szechynska-Hebda, J. Kruk, M. Gorecka, B. Karpinska, S. Karpinski, Evidence for light wavelength-specific photoelectrophysiological signaling and memory of excess light episodes in arabidopsis, Plant Cell 22 (2010) 2201–2218.
[6] R. Jennings, F. Garlaschi, G. Zucchelli, Light-induced fluorescence quenching in the light-harvesting chlorophyll *a*/*b* protein complex, Photosynth. Res. 27 (1991) 57–64.
[7] V. Barzda, R.C. Jennings, G. Zucchelli, G. Garab, Kinetic analysis of the light-induced fluorescence quenching in light-harvesting chlorophyll a/b pigment-protein complex of photosystem II, Photochem. Photobiol. 70 (1999) 751–759.
[8] W.I. Gruszecki, W. Grudzinski, M. Matula, P. Kernen, Z. Krupa, Light-induced excitation quenching and structural transition in light-harvesting complex II, Photosynth. Res. 59 (1999) 175–185.
[9] T.P.J. Kruger, V.I. Novoderezhkin, C. Ilioaia, R. van Grondelle, Fluorescence spectral dynamics of single LHCII trimers, Biophys. J. 98 (2010) 3093–3101.
[10] A.V. Ruban, R. Berera, C. Ilioaia, I.H. van Stokkum, J.T. Kennis, A.A. Pascal, H. van Amerongen, B. Robert, P. Horton, R. van Grondelle, Identification of a mechanism of photoprotective energy dissipation in higher plants, Nature 450 (2007) 575–578.
[11] T. Barros, W. Kuhlbrandt, Crystallisation, structure and function of plant light-harvesting Complex II, Biochim. Biophys. Acta Bioenerg. 1787 (2009) 753–772.
[12] T. Barros, A. Royant, J. Standfuss, A. Dreuw, W. Kuhlbrandt, Crystal structure of plant light-harvesting complex shows the active, energy-transmitting state, EMBO J. 28 (2009) 298–306.
[13] M.G. Muller, P. Lambrev, M. Reus, E. Wientjes, R. Croce, A.R. Holzwarth, Singlet energy dissipation in the photosystem II light-harvesting complex does not involve energy transfer to carotenoids, Chemphyschem 11 (2010) 1289–1296.
[14] N.E. Holt, D. Zigmantas, L. Valkunas, X.P. Li, K.K. Niyogi, G.R. Fleming, Carotenoid cation formation and the regulation of photosynthetic light harvesting, Science 307 (2005) 433–436.
[15] M. Wormit, P.H. Harbach, J.M. Mewes, S. Amarie, J. Wachtveitl, A. Dreuw, Excitation energy transfer and carotenoid radical cation formation in light harvesting complexes — a theoretical perspective, Biochim. Biophys. Acta 1787 (2009) 738–746.
[16] S. Amarie, J. Standfuss, T. Barros, W. Kuhlbrandt, A. Dreuw, J. Wachtveitl, Carotenoid radical cations as a probe for the molecular mechanism of nonphotochemical quenching in oxygenic photosynthesis, J. Phys. Chem. B 111 (2007) 3481–3487.
[17] S. Amarie, K. Arefe, J.H. Starcke, A. Dreuw, J. Wachtveitl, Identification of an additional low-lying excited state of carotenoid radical cations, J. Phys. Chem. B 112 (2008) 14011–14017.
[18] W.I. Gruszecki, R. Luchowski, M. Zubik, W. Grudzinski, E. Janik, M. Gospodarek, J. Goc, Z. Gryczynski, I. Gryczynski, Blue-light-controlled photoprotection in plants at the level of the photosynthetic antenna complex LHCII, J. Plant Physiol. 167 (2010) 69–73.
[19] W.I. Gruszecki, M. Zubik, R. Luchowski, W. Grudzinski, M. Gospodarek, J. Szurkowski, Z. Gryczynski, I. Gryczynski, Investigation of the molecular mechanism of the blue-light-specific excitation energy quenching in the plant antenna complex LHCII, J. Plant Physiol. 168 (2011) 409–414.
[20] P. Jahns, A.R. Holzwarth, The role of the xanthophyll cycle and of lutein in photoprotection of photosystem II, Biochim. Biophys. Acta (2011), doi:10.1016/j.bbabio.2011.1004.1012.
[21] Z. Krupa, N. Huner, J. Williams, E. Maissan, D. James, Development at cold-hardening temperatures. The structure and composition of purified rye light harvesting complex II, Plant Physiol. 84 (1987) 19–24.
[22] W.I. Gruszecki, M. Gospodarek, W. Grudzinski, R. Mazur, K. Gieczewska, M. Garstka, Light-induced change of configuration of the LHCII-bound xanthophyll (tentatively assigned to violaxanthin): a resonance Raman study, J. Phys. Chem. B 113 (2009) 2506–2512.
[23] J. Milanowska, W.I. Gruszecki, Heat-induced and light-induced isomerization of the xanthophyll pigment zeaxanthin, J. Photochem. Photobiol. B Biol. 80 (2005) 178–186.
[24] D. Niedźwiedzki, W.I. Gruszecki, Interaction between chlorophyll *a* and violaxanthin in different steric conformations. Model studies in monomolecular layers, Colloids Surf B Biointerfaces 28 (2003) 27–38.
[25] W. Grudzinski, M. Matula, J. Sielewiesiuk, P. Kernen, Z. Krupa, W.I. Gruszecki, Effect of 13-cis violaxanthin on organization of light harvesting complex II in monomolecular layers, Biochim. Biophys. Acta 1503 (2001) 291–302.
[26] R. Luchowski, S. Krawczyk, Stark effect spectroscopy of exciton states in the dimer of acridine orange, Chem. Phys. 293 (2003) 155–166.
[27] D. Olszowka, S. Krawczyk, W. Maksymiec, A study of molecular interactions in light-harvesting complexes LHCIIb, CP29, CP26 and CP24 by Stark effect spectroscopy, Biochim. Biophys. Acta 1657 (2004) 61–70.
[28] W. Liptay, Optical-absorption of molecules in liquid solutions in an applied external electric-field (electrochromism), Ber. Bunsen Ges. Phys. Chem. Chem. Phys. 80 (1976) 207–217.
[29] W. Liptay, B. Dumbache, H. Weisenbe, Effect of an electric field on optical molecular absorption. 7. Electrooptical and dielectrical measurements on some dyes, Z. Naturforsch. A Astrophys. Phys. Phys. Chem. A 23 (1968) 1601–1612.
[30] A. Strand, K. Kvernberg, A.M. Karlsen, S. Liaaen-Jensen, Geometrical E/Z isomers of (6R)- and (6S)-neoxanthin and biological implications, Biochem. Syst. Ecol. 28 (2000) 443–455.
[31] B. van Oort, A. van Hoek, A.V. Ruban, H. van Amerongen, Aggregation of light-harvesting complex II leads to formation of efficient excitation energy traps in monomeric and trimeric complexes, FEBS Lett. 581 (2007) 3528–3532.
[32] W.I. Gruszecki, E. Janik, R. Luchowski, P. Kernen, W. Grudzinski, I. Gryczynski, Z. Gryczynski, Supramolecular organization of the main photosynthetic antenna complex LHCII: a monomolecular layer study, Langmuir 25 (2009) 9384–9391.
[33] A.V. Ruban, D. Philip, A.J. Young, P. Horton, Carotenoid-dependent oligomerization of the major chlorophyll *a*/*b* light harvesting complex of photosystem II of plants, Biochemistry 36 (1997) 7855–7859.
[34] Y. Koyama, Y. Mukai, Excited states of retinoids, carotenoids and chlorophylls as revealed by time-resolved, electronic absorption and resonance Raman spectroscopy, in: R.J.H. Clark, R.E. Hester (Eds.), Biomolecular Spectroscopy, John Wiley & Sons Ltd., Chichester, 1993, pp. 49–137.
[35] P. Jahns, D. Latowski, K. Strzalka, Mechanism and regulation of the violaxanthin cycle: the role of antenna proteins and membrane lipids, Biochim. Biophys. Acta 1787 (2009) 3–14.
[36] Y. Miloslavina, A. Wehner, P.H. Lambrev, E. Wientjes, M. Reus, G. Garab, R. Croce, A.R. Holzwarth, Far-red fluorescence: a direct spectroscopic marker for LHCII oligomer formation in non-photochemical quenching, FEBS Lett. 582 (2008) 3625–3631.
[37] Z. Liu, H. Yan, K. Wang, T. Kuang, J. Zhang, L. Gui, X. An, W. Chang, Crystal structure of spinach major light-harvesting complex at 2.72 A resolution, Nature 428 (2004) 287–292.
[38] R. Standfuss, A.C.T. van Scheltinga, M. Lamborghini, W. Kuhlbrandt, Mechanisms of photoprotection and nonphotochemical quenching in pea light-harvesting complex at 2.5A resolution, EMBO J. 24 (2005) 919–928.
[39] M. Mozzo, L. Dall'Osto, R. Hienerwadel, R. Bassi, R. Croce, Photoprotection in the antenna complexes of photosystem II: role of individual xanthophylls in chlorophyll triplet quenching, J. Biol. Chem. 283 (2008) 6184–6192.
[40] R. Bensasson, E.A. Dawe, D.A. Long, E.J. Land, Singlet-triplet intersystem crossing quantum yields of photosynthetic and related polyenes, J. Chem. Soc. Faraday Trans. 73 (1977) 1319–1325.
[41] L. Dall'Osto, S. Cazzaniga, H. North, A. Marion-Poll, R. Bassi, The Arabidopsis aba4-1 mutant reveals a specific function for neoxanthin in protection against photooxidative stress, Plant Cell 19 (2007) 1048–1064.
[42] D. Niedzwiedzki, Z. Krupa, W.I. Gruszecki, Temperature-induced isomerization of violaxanthin in organic solvents and in light-harvesting complex II, J. Photochem. Photobiol. B Biol. 78 (2005) 109–114.
[43] S. Haferkamp, W. Haase, A.A. Pascal, H. van Amerongen, H. Kirchhoff, Efficient light harvesting by photosystem II requires an optimized protein packing density in grana Thylakoids, J. Biol. Chem. 285 (2010) 17020–17028.
[44] I. Rumak, K. Gieczewska, B. Kierdaszuk, W.I. Gruszecki, A. Mostowska, R. Mazur, M. Garstka, 3-D modelling of chloroplast structure under (Mg2+) magnesium ion treatment. Relationship between thylakoid membrane arrangement and stacking, Biochim. Biophys. Acta Bioenerg. 1797 (2010) 1736–1748.